COVER SHEET

Author version of the paper published as:
Rigby, P. A., Dobos, S. K., Cook, F. J. and Goonetilleke, A., 2006, 'Role of organic matter in framboidal pyrite oxidation', Science of the Total Environment, Vol. 367, pp. 847– 854.

Role of organic matter in framboidal pyrite oxidation

P.A Rigby [a], S. K Dobos [b], F. J Cook [c], A. Goonetilleke [a]

[a]School of Civil Engineering, Queensland University of Technology, GPO Box 2434 Brisbane QLD 4001, Australia.

Email: p.rigby@qut.edu.au Phone: (61 7) 3864 1544

[b]Dobos & Associates Pty Ltd, 6 Pandian Cresent Bellbowrie QLD 4070, Australia.

Email: sdobos@bigpond.net.au Phone: (61 7) 3202 6150 Fax: (61 7) 3202 6150

[c]CSIRO Land and Water, 120 Meiers Rd Indooroopilly QLD 4068, Australia.

Email: freeman.cook@csiro.au Phone: (61 7) 3214 2840 Fax: (61 7) 3214 2881

Abstract

An experimental system has been set up to investigate the reaction kinetics of framboidal pyrite oxidation in real, reactive acid sulfate soil assemblages. This study was undertaken to determine the degree to which pyrite oxidation rates are reduced by bacteriological reactions and organic matter, which both modify the net reaction mechanisms and compete for available oxygen. The results from these experimental runs not only confirm the role of organic matter in mitigating pyrite oxidation, but indicate that, at least initially, the acidity produced is consumed or otherwise ameliorated by parallel reactions. Tracking pH or $[H^+]$ in both a reactor and in soil does not accurately reflect reaction progress, and may not correctly indicate the true level of risk. In comparison, the tracking of pyrite oxidation with the concentration of sulfate in solution is not affected by side reactions or precipitation, and is therefore a better indicator for the rate of pyrite destruction.

Keywords: acid sulfate soils, framboidal pyrite oxidation, organic matter

1. Introduction

Low-lying coastal soils along the eastern Australian seaboard and elsewhere commonly contain variable amounts of both organic matter and iron sulfides, generally framboidal pyrite. (Low-lying is defined as <5 m Australian Height Datum HD, which is essentially mean sea level). The pyrite in these soils, if exposed to oxygen in air by excavation, dredging, stockpiling or by lowering of the water table through agricultural activities, drainage or drought, will oxidise to generate sulfuric acid and sulfate, hence their collective name 'acid sulfate soils'.

Increasing soil water acidity (decreasing pH) will increasingly corrode metal and concrete subsurface infrastructures, and will also generate increasing amounts of soluble aluminium and iron, which, if subsequently transported or released to receiving waters (Cook et al., 2000), can result in significant ecological impacts. It is therefore important that the potential risks to the environment are quantified and appropriate management strategies adopted to mitigate the adverse environmental impacts associated with any disturbance to acid sulfate soils.

Extensive guidance documents are available to facilitate the minimisation of environmental risk from acid sulfate soils (Dear et al., 2002). To date worst case scenarios based solely on the amount of pyrite in given volumes of soil have been the only means of quantifying acid production. This assumes that all the pyrite will be oxidized during a particular disturbance with no consideration of the rate of pyrite oxidation being taken into account (Ahern & Watling, 2000; Dear et al., 2002). There are only limited available data on the actual rates of 'in-situ' pyrite oxidation (Cook et al., 2002; Ward, 2002).

One management technique commonly employed involves neutralising the actual and/or potential soil acidity with alkaline material such as lime. The potential acidity is typically derived from the measured total pyrite concentration, but in many disturbances, not all the pyrite will be oxidised. By incorporating the rates of reaction into the determination of the amount of neutralising material required for a given disturbance, this may lead to a reduction in the quantities required. This in turn will reduce the wastage of energy resources and non renewable resources as well as reducing any environmental impacts that over-liming may cause.

The pyrite oxidation rate and hence acid generation rate, for a given volume of soil, depends in part on both the availability of dissolved oxygen reactant within the reaction volume and the reactive pyrite surface area. These are not sufficiently quantified by the analysis of pyrite content alone. A given mass of pyrite can have variable surface area (Lowson, 1982; Pugh et al., 1981), depending on the grainsize distribution and on grain morphology (crystal habit – cubes, octahedra, pyritohedra or raspberry shaped forms referred to as framboids).

The particle size and morphology of framboidal pyrite found in acid sulfate soils is very different from that used in previous laboratory studies (Bush & Sullivan, 1999; Rickard, 1973; Wilkin et al., 1996). Pyrite oxidation rates have been measured on pure mineral (non-framboidal) pyrite assemblages prepared within narrow grainsize ranges by various researchers (Table 1). These experiments and the derived pyrite oxidation rates laws cannot be applied to framboidal pyrite directly and hence acid sulfate soils generally, since the effects of grainsize and morphology are difficult to account for with sufficient precision.

The difficulties lie in the determination of grainsize distributions and reactive surface areas of framboidal pyrite in acid sulfate soils, as the framboids cannot be easily separated from the other fines; they are usually less than 70 μm in diameter (Weber, 2002).

The utilisation of these experiments to quantify pyrite oxidation rates in disturbed acid sulfate soils is further limited, as the soil organic matter and biological activity (bacterial respiration and growth) competes for available oxygen with pyrite (Inderatna & Blunden, 1999; Lloyd and Taylor, 1994; Nealson & Stahl, 1997).

The above two fundamental issues have been investigated on long-exposed cultivated (sugar cane) soil in a passive field study by Cook et al. (2002), but have not been addressed in detail and under experimental control. Consequently, our experiments and measurements are addressed to provide realistic acid sulfate soil reaction rates and mechanisms in the presence of natural organic matter and soil bacteria. The results will be more directly applicable for assessing realistic acid production risks, and hence environmental risks, in many cases involving excavations, disturbances and disposal of acid sulfate soils. In particular, this will enable better quantification of in-situ acid production rates, and hence better management protocols, in cases where excavation or agriculture lowers the water table in adjacent pyritic soils.

2. Materials and Methods

Figure 1 is a schematic diagram showing the experimental apparatus used in this study. An aqueous suspension consisting of pyritic fines and distilled water was continuously stirred in a reaction vessel, constructed from a vertically mounted Perspex column, 0.85 m in length and 0.2 m ID with a motor-driven stainless steel paddle mounted from above. A controlled air supply was continuously bubbled up through the reaction vessel throughout the course of the experiments, with the one exception noted below. High quality timber/wooden air stones, purchased from an aquarium store, were utilised to minimise bubble size as they produced considerably finer bubbles than the regular (ceramic) aquarium air stones.

The dissolved oxygen (DO), Redox potential (Eh) and pH of reactor solutions were continuously monitored, while air and water samples were taken periodically for analysis by Gas Chromatography (GC) and Inductively Coupled Plasma-Atomic Emission Spectroscopy (ICP AES). Head space gas compositions were analysed to identify any changes in O_2 and CO_2 concentrations, under the assumption that virtually all CO_2 produced would result from the consumption of O_2 by biological processes (bacteriological oxidation of organic matter) in the soil. Two experiments were performed under controlled room temperature conditions at 23 ± 1 °C, with a third experiment depicting larger temperature fluctuations (20 – 30 °C) common to the Queensland environment.

The various pyritic fines were collected during hydrosluiced fill placement at Lensworth's Kawana Waters development site on the Sunshine Coast of Queensland (26°43′06″S 153°06′04″E). In terms of solid phases,

the fines comprise dominant quartz, of grainsize range 70 to 0.2 μm, with lesser amounts of equally fine grained detrital minerals such as feldspars. Authigenic and/or detrital clays can be major constituents, followed by organic matter; pyrite is only a minor component of the fines (1-4 %).

A typical chemical analysis of the pyritic fines utilising X-Ray Florescence Spectroscopy (XRS) is given in Table 2. The components that are lost on ignition (LOI) are analysed separately by Leco Induction Furnace analysers which determine total carbon, nitrogen and sulfur. An inorganic carbon value was calculated from an acid neutralisation titration; since clays may partially neutralise acidity, this C value corresponds to a maximum carbonate content. Total Kjeldahl Nitrogen quantifies the amount of organic nitrogen plus ammonia/ammonium nitrogen. The chromium-reducible sulfur (Sullivan et al., 2000) component represents the sulfur content of the mineral pyrite, from which the total percentage of pyrite is calculated according to its stoichiometry. The pyrite content of the fines used in these experimental runs ranged from 1.9% to 3.3% by mass.

Semi-quantitative mineralogical compositions were characterised using X-ray Diffraction (XRD) and the SIROQUANT peak modelling package; a typical fines analysis is given in Table 3. Scanning Electron Microscopy (SEM) was utilised to investigate the micro-morphology of the pyrite in the soil fines, together with Energy Dispersive Spectroscopy (EDS) for mineral identification. The pyrite was found to be framboidal (Figure 2) with the overall grain size being generally less than 10 μm with infrequent framboidal sizes of up to 16 μm; only minor amounts of free-standing octahedra were observed.

The results presented in this paper were obtained from the first three experimental runs, of a larger set, designed to measure the degree by which pyrite oxidation in acid sulfate soils is limited by (diffusive) oxygen availability and further retarded by competition for available oxygen by organic matter and bacteriological activity. The first two runs had identical initial conditions, commencing with the same air supply rate (0.28 ± 0.04 cm^3 s^{-1}) and the same volume (1.3 litres) of reactive fines added to the aqueous mixture. The third experimental run, however, had approximately double the pyritic/reactive fines added to the system (2.9 litres).

3. Results and Discussion

The evolution of the three experimental runs is shown in Figure 3, which readily demonstrates the production of acid by the decreasing trend in the pH curves. Experiment 1 (Exp 1) however, had an interruption to the oxygen supply in the period from 50 to 100 hours. This is clearly reflected in the pH trace where at this scale the rate of pH decline (acid generation) quickly slowed down and then stopped. Once the oxygen supply was restarted, the pH decline continued at the same rate, indicating that once pyrite oxidation has commenced, the temporary removal of available oxygen has minimal effect on the overall oxidation rate.

All three curves display a consistent pattern in the fall of pH irrespective of the fact that two runs (Exp 1 & 2) commenced with much lower pyrite content (0.48 g/L) than the third (Exp 3) which commenced with 1.44 g/L of pyrite. All other variables were equal, with the same constant rate of oxygen supply (0.06 cm^3 s^{-1} O_2) for this initial period.

Ideally, the rate and hence amount of acid generated in the 'initial' part of the experiments, should be higher for Exp 3 than for the others, since it had over twice the reactive fines concentration (and hence higher reactive surface area). This supposition is corroborated by the trends in sulfate production depicted in Figure 4. In the 'initial' or earlier parts of the experiments, a higher sulfate production is actually observed for Exp 3 than that observed for Exp 2. Further evidence that would infer the production of higher acid generation rates for Exp 3 can be interpreted from DO concentrations in Exp 1 & 2 (excluding period of flow interruption in Exp 1) being consistently higher than those in Exp 3. This suggests that more O_2 was consumed in Exp 3 as a result of the higher pyrite content. Therefore if more O_2 was consumed due to pyrite oxidation this would lead to higher acid production. However, as all the experiments yielded very similar pH trends in the 'initial' period this indicates a degree of proton consumption, and that the ratio of proton production to consumption during the initial period is very similar in all cases.

It could therefore be argued that some of the H^+ ions are actually consumed during the course of the experiment by the remnant neutralisation capacity of the soils (including trace carbonate). Another potential sink for the removal of H^+ can occur from the sorption of H^+ ions by the clay particles in the soil (Sparks, 1995). A further possibility is that biological reactions could be taking place that consume H^+ ions.

The rate of oxidation in the 'later' section of the experiments, however, is dependent on the pyrite content, and final pH values clearly demonstrate that the total amount of acid produced is proportional to the pyrite content, as expected.

What is not apparent on the scale of Figure 3 is that while Exp 1 was underway there were rhythmic (laboratory) temperature fluctuations mirroring the temperature variations common to Queensland conditions. These are depicted in Figure 5 which shows an inverse relationship between the measured DO and the temperature of the aqueous soil suspension (period of oxygen supply interruption between 50-100 hrs not plotted), when the same constant feed of oxygen is supplied to the system.

Comparing experimental DO concentrations with the equilibrium dissolved oxygen (i.e. maximum DO in a non reactive system) clearly indicates that variations in the experimental DO are much greater than the variations in oxygen solubility alone. This important observation leads to a key issue relevant to pyrite oxidation in acid sulfate soils and two possible mechanisms for this amplified trend between temperature and DO.

The rate of pyrite oxidation will increase with temperature and can be calculated from the Arrhenius equation (e.g. Barrow, 1973). The experimental results, however, indicate oxygen consumption rates that are much higher than that for pyrite oxidation alone. Bacteriological reactions in soils can show even greater dependencies on temperature (Lloyd & Taylor, 1994). When these are calculated they indicate a doubling of reaction rate for the observed temperature rise. Consequently the observed temperature – DO relationship can be explained by increased rates of bacteriological and pyrite oxidation reactions, with the former more dominant.

Further evidence of soil respiration/bacteriological oxidation of organic matter is apparent in the head space gas compositions found above the stirred soil suspensions. Gas samples were taken at various intervals during the experimental runs Exp2 and Exp3. Three replicates were taken at each sampling time and the averages are presented in Table 4. The increase in CO_2 concentrations from standard atmospheric conditions (Glinski & Stepniewski, 1985) clearly identifies that soil respiration is occurring in the reaction vessel.

Figure 6 shows an expanded scale of the section of interrupted air supply to Exp 1 which commenced at approximately 50 hours into the experimental run. No air flowed for approximately 50 hours and a continuous decrease in DO is clearly apparent, with complete consumption of all available oxygen (DO) in the system after approximately 24 hours. Assuming all the oxygen in the reaction vessel was consumed by pyrite oxidation; the pH change with time can be calculated using the appropriate stoichiometry (Evangelou, 1995; Singer & Stumm, 1970; Stumm & Morgan, 1981) and is illustrated in Figure 6. This calculation does not involve a rate equation, rather it utilises the observed decrease in oxygen concentration to calculate a theoretical acid generation assuming no other reactions compete for oxygen. Very clearly the observed pH and the calculated pH change are very different.

The above observations, however, have been made with the additional assumption that pyrite destruction can be represented by acid production (i.e. H^+ ions produced in the reaction are conserved). If this assumption is correct then the maximum percentage of available oxygen consumed by pyrite during this period is calculated to be 0.2%, as apposed to the usual conservative assumption of 100% oxygen consumed by pyrite oxidation.

As mentioned earlier, however, it is argued that some of the H^+ ions are actually consumed during the course of the experiment. Therefore the percentage of O_2 consumed by pyrite oxidation would be higher than that previously calculated from Figure 6. It could therefore be hypothesized that although the percentage of oxygen consumption will be greater than 0.02% it will still be much lower than the conservative assumption of 100%. Sulfate production, however, is generally considered to be a conservative estimator of pyrite destruction.

If we again consider Figure 4, which shows the increase in sulfate (SO_4^{2-}) concentrations with time for Exp 2 and Exp3, measured using ICP AES analysis. It was assumed that all sulphur present was in the form of SO_4^{2-} and consequently that all sulfur measured using ICP AES was therefore SO_4^{2-}. This assumption was based on previous research on pyrite oxidation (Goldhaber, 1983; Moses et al., 1987; Nordstrom, 1982; Williamson & Rimstidt, 1994) which generally agrees that sulfate is the stable sulfur oxidation product in acidic solutions when there is excess oxygen available. From Figure 4 it can be seen that the rate of sulfate production for Exp 3 is considerably greater than that for Exp 2, reflecting higher pyrite concentration and reactive surface area.

Utilising these sulfate concentrations, corresponding H^+ concentrations were calculated using the appropriate stoichiometry (Evangelou, 1995; Singer & Stumm, 1970; Stumm & Morgan, 1981) and then converted to pH values. These predicted values of pH again assume that the H^+ ions generated are conserved. When comparing the measured and calculated pH plots (Figure 7), it is clearly apparent that the rate of decrease in calculated pH is greater than that observed in the experimental runs, again suggesting that H^+ are consumed during the course of the experiments.

4. Conclusions

The results from these experiments clearly indicate the important role of bacteriological activity and organic matter which both compete with pyrite for available DO. The comparison of H^+ and sulfate generation rates with instantaneous DO values and head space gas compositions indicate unequivocally that organic matter and/or bacteriological reactions consume large amounts of available DO from soil water. In so doing, in any ‘oxygen limited’ soil, they significantly retard both the rate and amount of generated acid.

In tracking the reactions in the experimental soil suspensions it is clear that sulfate rather than generated H^+ should be used as indicators of reaction progress (conservative). The apparent dynamic equilibria observed in replicate experiments indicate a consistency in reaction mechanisms which will require the tracking of ferrous and ferric ion concentrations in solution and changes in the relative amounts of O_2 and CO_2 outputs from the reactor for given O_2 inputs. Experiments now under way, that are tracking outflow gas volumes as well as compositions, will enable formal quantification of the ratio of oxygen consumed by pyrite to that consumed by organic matter and microbiotic reactions.

This paper has not addressed in any detail the application of published intrinsic pyrite oxidation rates to framboidal pyrites which have substantially higher unit surface areas than hard-rock coarser pyrite crystals. With further refinement of the apparatus however, ensemble reaction rates for real soil fines, and real acid sulfate soils, will be generated.

The results of this work will be applied directly in the assessment of acid risk, and the quantification of likely acid production from earthworks and other excavations that require disturbance of acid sulfate soils. To date worst case scenarios based purely on the amount of pyrite in given volumes of soil have been the only means of quantifying acid production based on the assumption that all the pyrite will be oxidized during a particular disturbance. Data from these experiments may be pivotal in establishing that only limited acid risk will arise in given proposed excavations as the pyrite oxidation is rate limited, and further retarded by low oxygen availability and competition for oxygen by organic matter and bacteriological activity.

Furthermore, without realistic data, reaction mechanisms and rates, worst-case scenarios need to be assumed for the management of acid sulfate soil disturbances and can result in excessive amelioration treatments. The resulting environmental impacts would include wastage and depletion of non renewable resources and the potential for soluble and unused alkaline materials leaching into the surrounding waterways or groundwater, causing ecological changes that may not be reversible in systems already under stress from urbanisation.

Acknowledgements

This research project was funded by a QUT Post Doctoral Research Fellowship. Further assistance from Lensworth Kawana Waters Pty Ltd is appreciated.

References

Ahern CR, Watling KM. Basic management principles: Avoidance, liming, burial. In: Ahern CR, Hey KM, Watling KM, Eldershaw VJ, editors. Acid Sulfate Soils: Environmental Issues, Assessment & Management, Technical Papers. Brisbane, 20-22 June, 2000. Department of Natural Resources, Indooroopilly, Qld, Australia.

Barrow GM. Physical Chemistry. McGraw-Hill, Inc, 1973, 787pp.

Bush RT, Sullivan LA. Pyrite morphology in three Australian Holocene sediments. Australian Journal of Soil Research, 1999; 37: 637-653.

Cook FJ, Hicks W, Gardner EA, Carlin GD, Froggatt DW. Export of acidity in drainage water from acid sulfate soils. Marine Pollution Bulletin, 2000; 41: 319-326.

Cook FJ, Carlin GD, Dobos SK, Millar GE. Oxidation rate of pyrite in acid sulfate soils: In situ measurements and modelling. In: The 5th International Acid Sulfate Soil Conference. Tweed Heads, NSW, 25-30 August, 2002.

Dear SE, Moore NG, Dobos SK, Watling KM, Ahern CR. Soil management guidelines. In: Queensland acid sulfate soil technical manual. Department of Natural Resources and Mines, Indooroopilly, Queensland, Australia, 2002.

Evangelou VP. Pyrite oxidation and its control. CRC Press, 1995, 293pp.

Glinski J, Stepniewski W. Soil aeration and its role for plants. CRC Press, Boca Raton, Florida, 1985.

Goldhaber MB. Experimental study of metastable sulfur oxyanion formation during pyrite oxidation at pH 6-9 and 30C. American Journal of Science, 1983, 283, 193-217.

Indraratna B, Blunden B. Nature and properties of acid sulphate soils in drained coastal lowlands in New South Wales. Australian Geomechanics Journal, 1999, 34(1), 61-78.

Kamei G, Ohmotoh H. The kinetics of reactions between pyrite and O_2-bearing water revealed from in situ monitoring of DO, Eh and pH in a closed system. Geochimica et Cosmochimica Acta, 2000; 64(15): 2585-2601.

Lloyd J, Taylor JA. On the temperature dependence of soil respiration. Functional Ecology, 1994; 8: 315-323.

Lowson RT. Aqueous pyrite oxidation by molecular oxygen. Chemical Reviews, 1982, 82, 461-497.

McKibben M, Barnes H. Oxidation of pyrite in low temperature acidic solutions: Rate laws and surface textures. Geochimica et Cosmochimica Acta, 1986; 50: 1509-1520.

Moses CO, Herman JS. Pyrite oxidation at circum-neutral pH. Geochimica et Cosmochimica Acta, 1991; 55: 471-482.

Moses CO, Nordstrom DK, Herman JS, Mills AL. Aqueous pyrite oxidation by dissolved oxygen and by ferric iron. Geochimica et Cosmochimica Acta, 1987; 51: 1561-1571.

Nealson KH, Stahl DA. Microorganisms and biogeochemical cycles: What we can learn from layered microbial communities? In: Banfield JF, Nealson KH, editors. Geomicrobiology: Interactions between microbes and minerals, Reviews in Mineralogy, 1997, 35.

Nicholson RV, Gillham RW, Reardon EJ. Pyrite oxidation in carbonate-buffered solution: 1. Experimental kinetics. Geochimica et Cosmochimica Acta, 1988; 52: 1077-1085.

Nordstrom DK. Chapter 3. Aqueous pyrite oxidation and the consequent formation of secondary iron minerals. In: Kittrick JA, Fanning DS, Hossner LR, editors. Acid Sulphate Weathering. Special Publication No. 10. Soil Science Society of America, Madison, Wisconsin, 1982, 37-56.

Pugh CE, Hossner LR, Dixon JB. Pyrite and marcasite surface area as influenced by morphology and particle diameter. Soil Science Society of America Journal, 1981, 45, 979-982.

Rickard DT. Sedimentary iron sulphide formation. In: Dost H, editor. Acid Sulphate Soils. Proceedings of the International Symposium on Acid Sulphate Soils. Wageningen, The Netherlands., 13-20 August, 1972. 1. International Institute for Land Reclamation and Improvement, 1973; Publication 18: 28-65.

Singer PC, Stumm W. Acidic mine drainage: the rate-determining step. Science, 1970.

Sparks DL. Environmental Soil Chemistry. Academic Press, Inc., 1995.

Stumm W, Morgan JJ. Aquatic chemistry. An introduction emphasizing chemical equilibria in natural waters. John Wiley & Sons, 1981, 469-472.

Sullivan LA, Bush RT, McConchie D, Lancaster G, Clark MW, Lin C, Saenger P. Chromium reducible sulfur - Method 22B. In: Ahern CR, Hey KM, Watling KM, Eldershaw VJ, editors. Acid Sulfate Soils: Environmental Issues, Assessment & Management, Technical Papers. Brisbane, 20-22 June, 2000. Department of Natural Resources, Indooroopilly, Qld, Australia.

Ward NJ, Sullivan LA, Bush RT. Sulfide oxidation and acidification of acid sulfate soil materials treated with CaCO3 and seawater-neutralised refinery residue. Australian Journal of Soil Research, 2002, 40, 1057-1067.

Weber PA, Skinner WM, Smart RSC, Thomas JE. Influence and management of iron carbonates and framboidal pyrite during ANC titration type tests. In: Minerals Council of Australia's 2002 Sustainable Development Conference. New Castle, 2002, 268-283.

Wilkin RT, Barnes HL, Brantley SL. The size distribution of framboidal pyrite in modern sediments: An indicator of redox conditions. Geochimica et Cosmochimica Acta, 1996; 60(20): 3897-3912.

Williamson MA, Rimstidt JD. The kinetics and electrochemical rate-determining step of aqueous pyrite oxidation. Geochimica et Cosmochimica Acta, 1994; 58(24): 5443-5454

Table 1. Experimental investigations of intrinsic pyrite oxidation rates

Mineral Pyrite Grainsize (μm)	Reference
74-177	Kamei & Ohmotoh, 2000
125-250	McKibben & Barnes, 1986
38-45 180-212 500-600	Moses et al., 1987
38-45	Moses & Herman, 1991
54, 108, 215	Nicholson et al., 1988
150-250	Williamson & Rimstidt, 1994

Table 2. Typical chemical analysis of the pyritic fines

Soil Components	Weight %
SiO_2	56.30
TiO_2	1.38
Al_2O_3	16.40
Total Fe as Fe_2O_3	7.80
MnO	0.04
MgO	1.20
CaO	0.97
SrO	0.01
Na_2O	0.71
K_2O	1.14
P_2O_5	0.12
LOI at 1,000 ^oC	13.00
C Total	3.58
C Inorganic	0.09
Total Kjeldahl Nitrogen	0.07
S Total	1.91
Chromium reducible S	1.50

Table 3. Typical mineral compositions of the pyritic fines

Mineral Phases	Weight %
Quartz SiO_2	24.6
Kaolinite $Al_2Si_2O_5(OH)_4$	29.2
Plagioclase feldspar solid solution (Albite $NaAlSi_3O_8$ and Anorthite $CaAlSi_2O_8$)	2.5
Alkali feldspars (K, Na) $AlSi_3O_8$	0.9
Pyrite FeS_2	3.1
Montmorillonites	1.4
Gypsum $CaSO_4.2H_20$	1.2
Unresolvable plus amorphous content	33.2

Table 4. Head space gas compositions

Elapsed Time (hours)	Gas Concentrations (% Volume)		
	N_2	O_2	CO_2
Exp 2.			
184	75.86	19.22	0.76
241	69.52	18.62	0.78
328	69.87	18.56	0.74
Exp 3.			
19	72.96	16.57	1.25
110	61.64	12.25	0.94
135	64.12	10.72	0.66
377	84.58	7.18	0.75
430	81.07	18.56	0.36
504	80.73	18.66	0.60
Std. Atmos.[a]	76.29	20.47	0.03

[a] Standard atmospheric gas compositions shown for reference

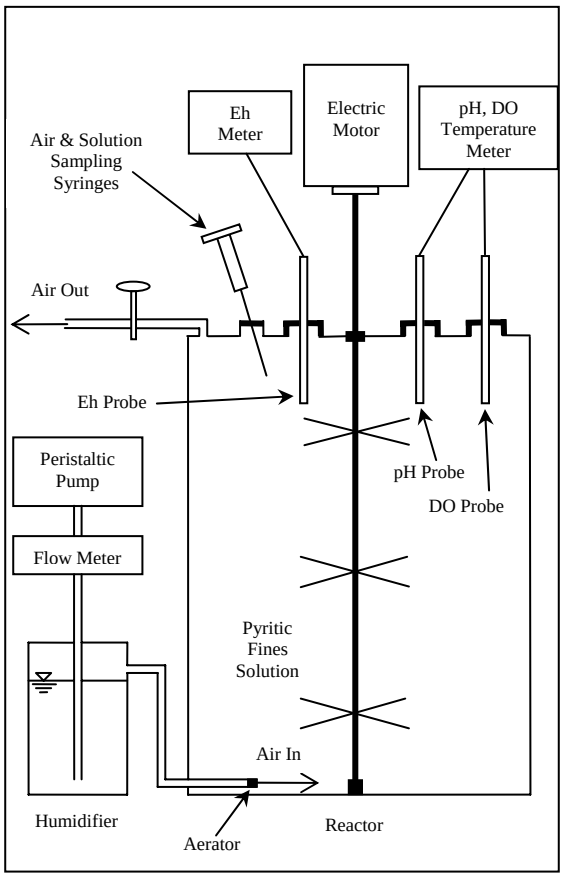

Figure 1. Schematic of experimental setup.

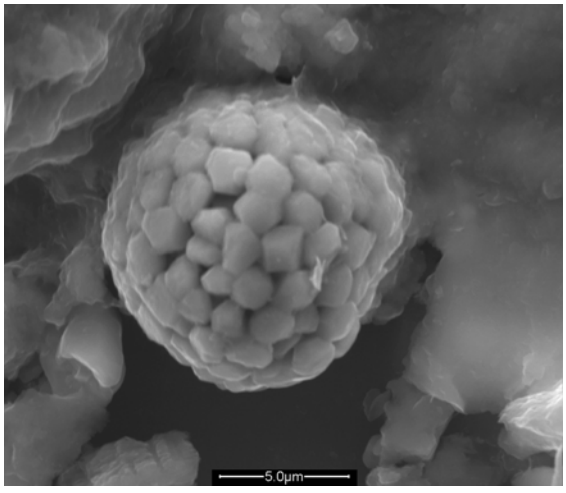

Figure 2. SEM photograph of framboidal pyrite.

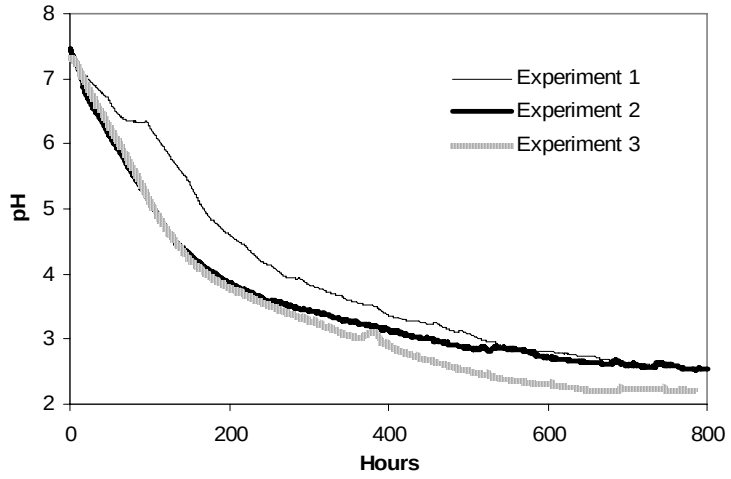

Figure 3. pH change with time for all experimental runs.

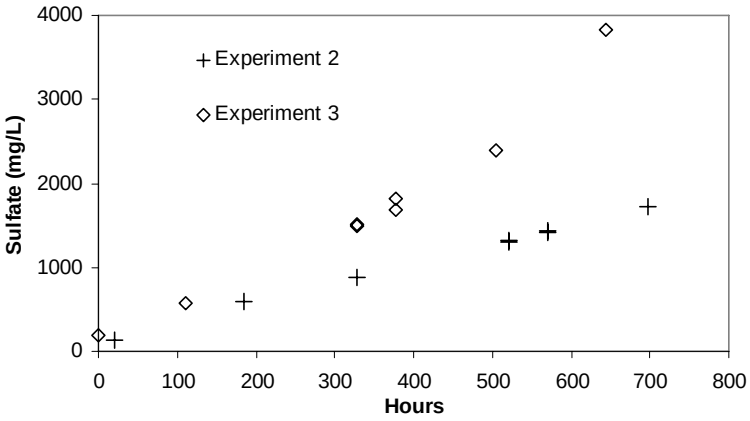

Figure 4. Sulfate concentrations for Exp 2 & 3.

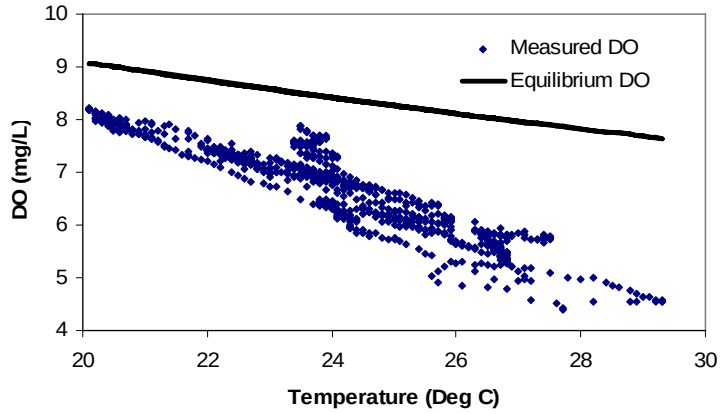

Figure 5. DO and temperature fluctuations in Exp 1. The equilibrium DO for a non reactive system is illustrated for reference.

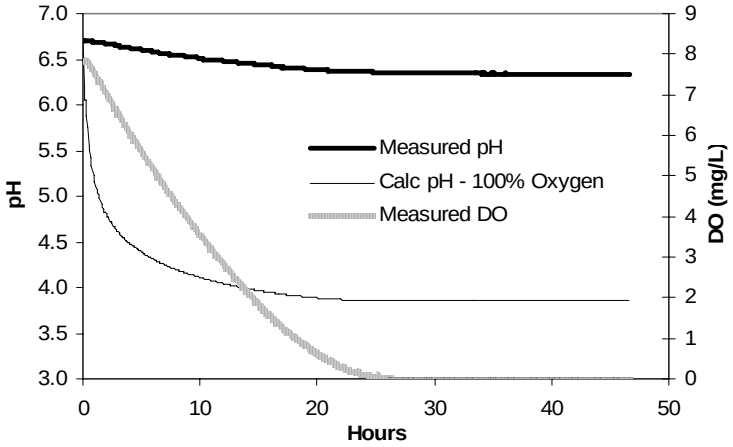

Figure 6. Measured DO and pH together with calculated pH change (Calc pH assumes 100% available oxygen consumed by pyrite oxidation, via ferric oxide, to ferrous iron plus sulfate) for the section of interrupted air flow in Exp 1.

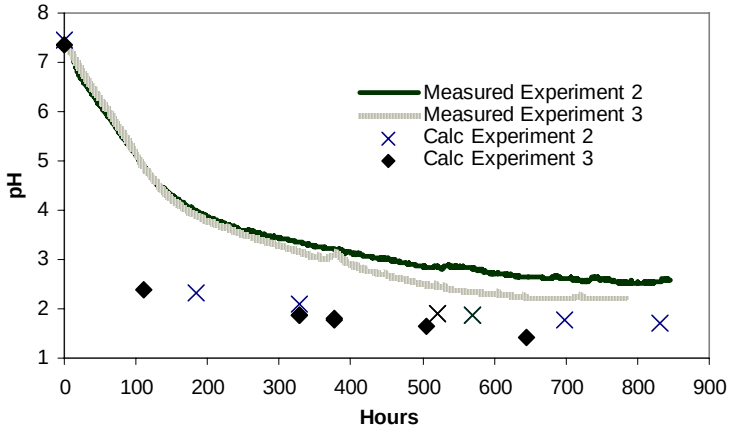

Figure 7. Measured pH and calculated pH from ICP sulfate concentrations for Exp 2 & 3.